Miner Petrol
DOI 10.1007/s00710-012-0200-3

ORIGINAL PAPER

Zircon geochronology, elemental and Sr-Nd isotope geochemistry of two Variscan granitoids from the Odenwald-Spessart crystalline complex (mid-German crystalline rise)

W. Siebel · S. Eroğlu · C. K. Shang · J. Rohrmüller

Received: 29 August 2011 / Accepted: 20 April 2012

Abstract The crystalline parts of the Bergsträsser (western) Odenwald and the southern Spessart expose Variscan I-type granitoids of the mid-German crystalline rise that formed during subduction of the Rheic ocean and collision of Avalonia and Armorica about 365 and 330 Ma ago. We present geochemical, Sr-Nd isotopic, single zircon $^{207}Pb/^{206}Pb$ evaporation and conventional U-Pb data from a diorite-granodiorite complex of the southern Spessart and from a flasergranitoid of the Bergsträsser Odenwald unit II. Both intrusions provide almost identical zircon ages (332.4±1.6 Ma for Odenwald and 330.4± 2.0 Ma for Spessart). Lack of inherited or pre-magmatic zircon components connotes magma genesis in deep crustal hot zones despite low temperature estimates (758–786 °C) derived from zircon saturation thermometry. Investigated rock samples display normal- to high-K calc-alkaline metaluminous (Spessart) and weakly peraluminous (Odenwald) geochemical characteristics. The Spessart pluton has lower $\varepsilon Nd_{(T)}$ values (−2.3 to −3.0) and higher $^{87}Sr/^{86}Sr_i$ ratios (0.7060 to 0.7066) compared to Odenwald flasergranitoid ($\varepsilon Nd_{(T)}$=−0.8 and $^{87}Sr/^{86}Sr_i$=0.7048). In terms of the tectonic setting, the diorite-granodiorite complex of the southern Spessart forms the continuation of the north Armorican arc segment exposed in the Bergsträsser Odenwald. Taking into account previously reported geochemical and isotopic results, it is concluded that the Spessart pluton does not match compositions of Odenwald unit II granitoids but likely represents the north-eastward extension of unit III.

Editorial handling: A. Möller

W. Siebel (✉) · S. Eroğlu · C. K. Shang
Fachbereich Geowissenschaften,
Wilhelmstraße 56,
72074 Tübingen, Germany
e-mail: wolfgang.siebel@uni-tuebingen.de

J. Rohrmüller
Bayerisches Landesamt für Umwelt,
95615 Marktredwitz, Germany

Introduction and aims of investigation

In the Variscan orogen of central Europe clear recognition of plate boundary magmatism is complicated by widespread occurrence of late-orogenic anatectic granitoids, which are randomly distributed throughout the orogen (Finger et al. 1997; Schaltegger 1997; Siebel 1998). Granitoids of arc-affinity (i.e., those with calc-alkaline intermediate to basic compositions), however, have been documented in a number of basement units (Odenwald, Massif Central, southern Black Forest, Bohemian Massif, western Carpathian Mts.) and the recognition of ancient plate boundary magmatism was an essential step in working out new plate tectonic models for the central European Variscides (Hann et al. 2003; Liew and Hofmann 1988; Pin and Paquette 2002; Poller et al. 2000; Shaw et al. 1993; Žák et al. 2010).

A well defined zone of arc granitoids occurs along the strike of the mid-German crystalline rise (MGCR, Altherr et al. 1999; Anthes and Reischmann 2001; Zeh et al. 2005; Zeh and Will 2010). This zone represents the plate boundary between the basement of central Europe, often referred to as Armorica or Armorican Terrane Assemblage, and the microcontinent Avalonia (Franke 2000; Stampfli et al. 2002; Linnemann et al. 2004). Ancient arc magmas of the MGCR are well-exposed in the northern Vosges, the Palatinate Forest and the Bergsträsser Odenwald and similar remnants are also preserved in the southern Spessart and the Kyffhäuser (Fig. 1). This paper presents new compositional and isotope data for a flasergranitoid from the Bergsträsser Odenwald and for a diorite-granodiorite intrusion from the southern Spessart situated ~50 km to the northeast. This area

Published online: 13 May 2012

is composed of two plate fragments with different tectonic identity (Oncken 1997). The eastern Odenwald (Böllstein Odenwald or unit IV, see below) and the central Spessart gneiss dome represent a tectonic window exposing Avalonian footwall rocks, whereas the Bergsträsser Odenwald and the southern Spessart crystalline basement are part of the north Armorican plate margin (Fig. 1). It has also been shown that granitoids from different regional or tectonic units of the western (Bergsträsser) Odenwald have specific petrological, textural or geochemical characteristics (Henes-Klaiber 1992; Altherr et al. 1999). Here we explore the question to which extend are igneous rocks from the Spessart genetically related to any of the units from the Bergsträsser Odenwald.

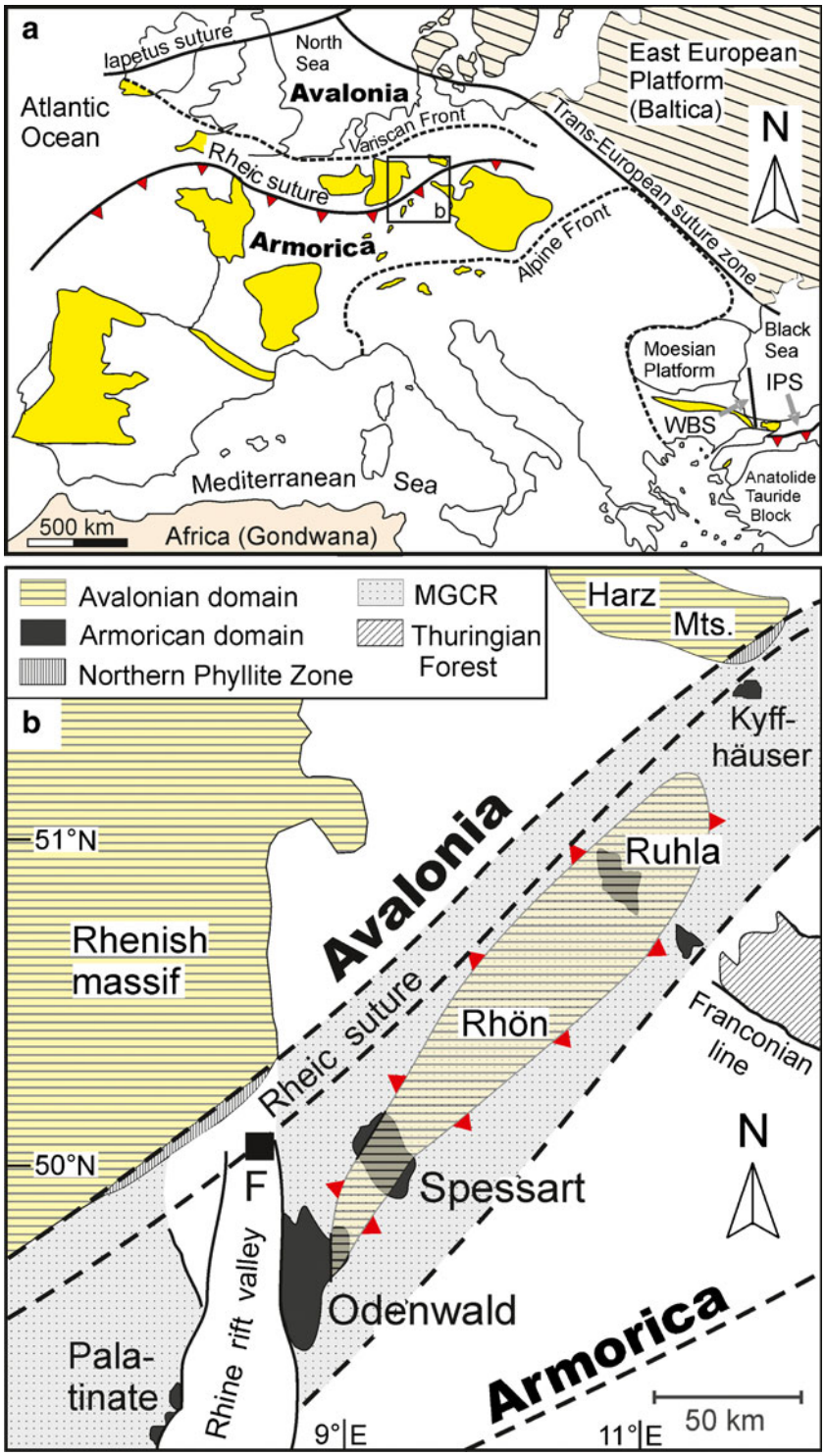

Fig. 1 **a** Tectonic map of Europe showing Variscan units and trace of the Rheic suture (modified after Okay et al. 2011). Shaded (*yellow*) zones indicate relics of the Variscan mountain chain. *IPS* Intra Pontide Suture, *WBS* West Black Sea Fault; **b** Location map of the mid-German crystalline rise (MGCR) modified after Oncken (1997) and Kroner et al. (2008) with Rheic suture located along the Northern Phyllite zone (Franke 2000). *F* Frankfurt

Geological setting and previous geochronology

The most widely accepted model of the MGCR is that it has formed by southward subduction (Liew and Hofmann 1988) of the Rheic ocean (McKerrow and Ziegler 1972). The Rheic ocean developed by separation of Avalonia from Gondwana during the Ordovician (Stampfli et al. 2002; Nance et al. 2010). The final closure of the Rheic ocean during the Lower Carboniferous led to oblique Variscan collision between Avalonia (meanwhile part of the southern margin of Laurussia) and Gondwana and this collision involved ongoing magmatism in the intervening Armorican microplate. The MGCR constitutes the north-westernmost part of the Saxothuringian lithostratigraphic unit which mainly represents Armorican type crust but also contains underplated slivers of Avalonia (Oncken 1997, 1998) (Fig. 1). To the north, the curvilinear MGCZ is bordered by the Northern Phyllite zone with outcrops at the southern border of the Rhenish Massif and the Harz Mts. (Fig. 1). The area between theses units defines the intricate, in part cryptic, Rheic suture (Timmerman 2008) (Fig. 1). To the west and to the east, this suture is displaced along strike-slip faults and possibly re-emerges within the Armorican Massif (Faure et al. 2010) and, as Intra-Pontide suture (IPS), in NW Turkey (Okay et al. 2006, 2011) (Fig. 1a).

The accretion model implies that the MGCR hosts units from the footwall (Avalonia) and from the hanging wall (Armorica) of the Rheic suture (Oncken 1997, 1998). Allochtonous footwall rocks occur in the central Spessart crystalline and the eastern Odenwald (Böllstein Odenwald, or unit IV) whereas in the southern Spessart and the western (Bergsträsser) Odenwald metamorphic and igneous rocks of the hanging wall are exposed (Fig. 1b). Rocks of the hanging wall underwent Late Carboniferous (342–332 Ma) thermal peak metamorphism under Abukuma-type facies conditions (Todt et al. 1995; Will and Schmädicke 2001, 2003). On the other hand, lenses of retrogressed eclogite, embedded in garnet-bearing orthogneisses of the Böllstein Odenwald, indicate a minimum age of 357±6 Ma (Lu-Hf whole-rock garnet) for the high pressure facies event in the footwall unit (Scherer et al. 2002; Will and Schmädicke 2001, 2003). Both units (Böllstein and Bergsträsser Odenwald) were welded together between 320 and 330 Ma along the NNE striking Otzberg fault zone (Schälicke 1975, Fig. 2).

Magmatism in the upper plate of the MGCR (Bergsträsser Odenwald and southern Spessart) lasted from Late-Devonian to Early Carboniferous times. The Bergsträsser Odenwald is generally subdivided into three geotectonic units (units I-III from north to south, Fig. 2), likely to be juxtaposed tectonically, as evidenced by different HT-LP assemblages (Willner et al. 1991; Krohe 1992, 1996). Towards the west, these units

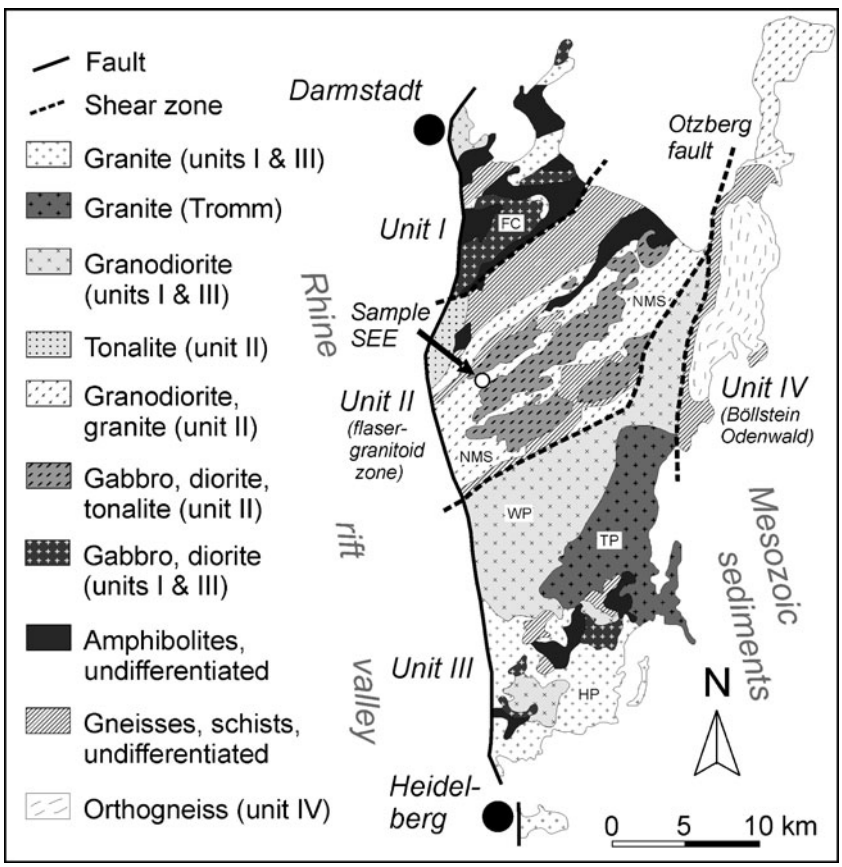

Fig. 2 Simplified geological map of the Odenwald crystalline complex (modified after Altherr et al. 1999; Krohe 1996) with main geological units I–IV and location of flasergranitoid sample *SEE* in unit II. Abbreviations: *FC* Frankenstein complex, *HP* Heidelberg pluton, *NMS* Neunkirchen magmatic suite, *TP* Tromm pluton, *WP* Weschnitz pluton

are bounded by the Rhine rift valley, whereas to the east they are cut by the Böllstein Odenwald or covered by younger Mesozoic sedimentary strata. More than 80 % of the exposed basement units consist of granitoid rocks. Unit I comprises the Frankenstein complex, made up of gabbroic rocks and granites (Kreher 1994). Unit II, also referred to as flasergranitoid zone (Nickel and Maggetti 1974; Stein 2000), is composed of intermediate and felsic granitoids including diorites, quartzdiorites, granodiorites, tonalites and granites, whereas in unit III (southern Bergsträsser Odenwald) granodiorites and granites (e.g., Weschnitz, Tromm, Heidelberg) are the prevailing rock-types (Fig. 2). It is generally assumed that the large geochemical variation within the flasergranitoid zone (unit II) resulted from successive intrusion of contrasting magma batches rather than from in-situ fractional crystallization of single magma bodies. According to Stein (2000, 2001a) the emplacement of these granitoids is best explained by the nested diapir model (Allen 1993; Paterson and Vernon 1995) that assumes successive magma ascent by the rise of several large magma batches.

Age data reveal older emplacement ages for granitoids from unit I (362±7 Ma, $^{207}Pb/^{206}Pb$ zircon age of the Frankenstein gabbro, Kirsch et al. 1988) and *c*. 25 Ma younger ages for those of units II and III (338–330 Ma and 336–326 Ma, resp.; K-Ar ages on hornblende and biotite, Kreuzer and Harre 1975; Schubert et al. 2001). Besides, there is a gradual change in rock composition from more mafic granitoids in unit I through intermediate rocks in unit II towards more felsic rocks in unit III (Henes-Klaiber 1992; Altherr et al. 1999). These temporal and compositional variations were explained by (1) north–south migration of the volcanic front as a result of subduction erosion and underplating (Oncken 1997) and (2) transition from subduction related arc magmatism to syn-collisional crustal thickening (Altherr et al. 1999). Confining pressure estimates using various geobarometric methods (Altherr et al. 1999; Henes-Klaiber 1992; Willner et al. 1991) suggest that the plutons emplaced at pressures in the range of 1–3 kbar in unit I and 4–6 kbar in units II and III.

The Spessart crystalline complex (Fig. 3) consists of a series of north-east striking geological formations with different lithological characteristics (see Hirschmann and Okrusch 2001 for review on subdivision of lithostratigraphic units). From analyses of deep seismic reflection data obtained from the DEKORP 2 S line it was inferred that these formations define a dome-like antiform (Behr and Heinrichs 1987; Weber 1995). This antiform is subdivided into two major tectonic units (Fig. 3). The lower tectonic unit, occupying the central part of the Spessart basement, contains Avalonia-type crust. It is composed of upper greenschist- to amphibolite-facies metasediments and paragneisses. The rocks of the lower tectonic unit were intruded by 418±10 and 410±18 Ma old granites and granodiorites ($^{207}Pb/^{206}Pb$ zircon evaporation ages; Dombrowski et al. 1994, 1995). The plutons were later transformed into orthogneisses and are divided in S-type (red gneisses) and transitional S-I type (Haibach gneiss) rocks (Lippolt 1986; Okrusch and Richter 1986; Nasir et al. 1991; Dombrowski et al. 1995). In terms of age and composition they resemble those from the Böllstein Odenwald suggesting a genetic link between both units. The upper tectonic unit is preserved in the northwestern and southeastern parts of the Spessart Mts. and is made up of amphibolites and amphibolite-facies biotite and hornblende gneisses. In the northwest, the upper unit is separated by the inferred Michelbach thrust from underlying upper-greenschist facies formations whereas in the southeast the contact between the upper and lower tectonic unit is supposed to be defined by a high-temperature mylonite zone (Weber 1995) (Fig. 3). Hanging wall igneous rocks equivalent to the Bergsträsser granitoids occur in the southernmost part of the exposed Spessart basement and are generally referred to as diorite or diorite-granodiorite complex (Braitsch 1957a, b; Okrusch 1963). Long controversy existed over the origin of this complex which now is regarded as an igneous intrusive body (for recent summary, see Okrusch et al. 2011). Textural features and the presence of numerous mafic (amphibolitic) enclaves are largely consistent with an origin of the diorite-granodiorite complex as commingled mafic magma. Towards the northwest the magmatic complex is bordered by the Elternhof paragneiss formation (Fig. 3) and this boundary probably represents the original intrusive contact between the pluton and the country rocks (Braitsch 1957a, b). Planar fabrics intensifying towards this contact (Okrusch et al. 2011) are considered as syntectonic and might have been produced by expansion of the pluton during emplacement. A late Variscan age of the diorite-granodiorite complex was already proposed by Bederke (1957) and two samples from the quarry "Am Stengerts" dated prior to this study, gave an average U-Pb zircon age of 329.6±0.8 Ma (Anthes and Reischmann 2001) and a K-Ar amphibole age of 328±4 Ma (Nasir et al. 1991).

Rock samples and structural characteristics

Geochemical and isotopic data were acquired for the Spessart diorite-granodiorite complex (samples *HB*) and an Odenwald flasergranitoid (sample *SEE*) of unit II. The diorite-granodiorite complex was sampled at four different localities (for sample locations see Table 1 and Figs. 2 and 3). All samples are largely undeformed and, with the exception of sample *HB-4*), unaltered and show magmatic fabrics. In places, heterogeneous schlieren texture, defined by K-feldspar or biotite aggregates, which was ascribed to magmatic foliation (Anthes and Reischmann 2001), can be observed.

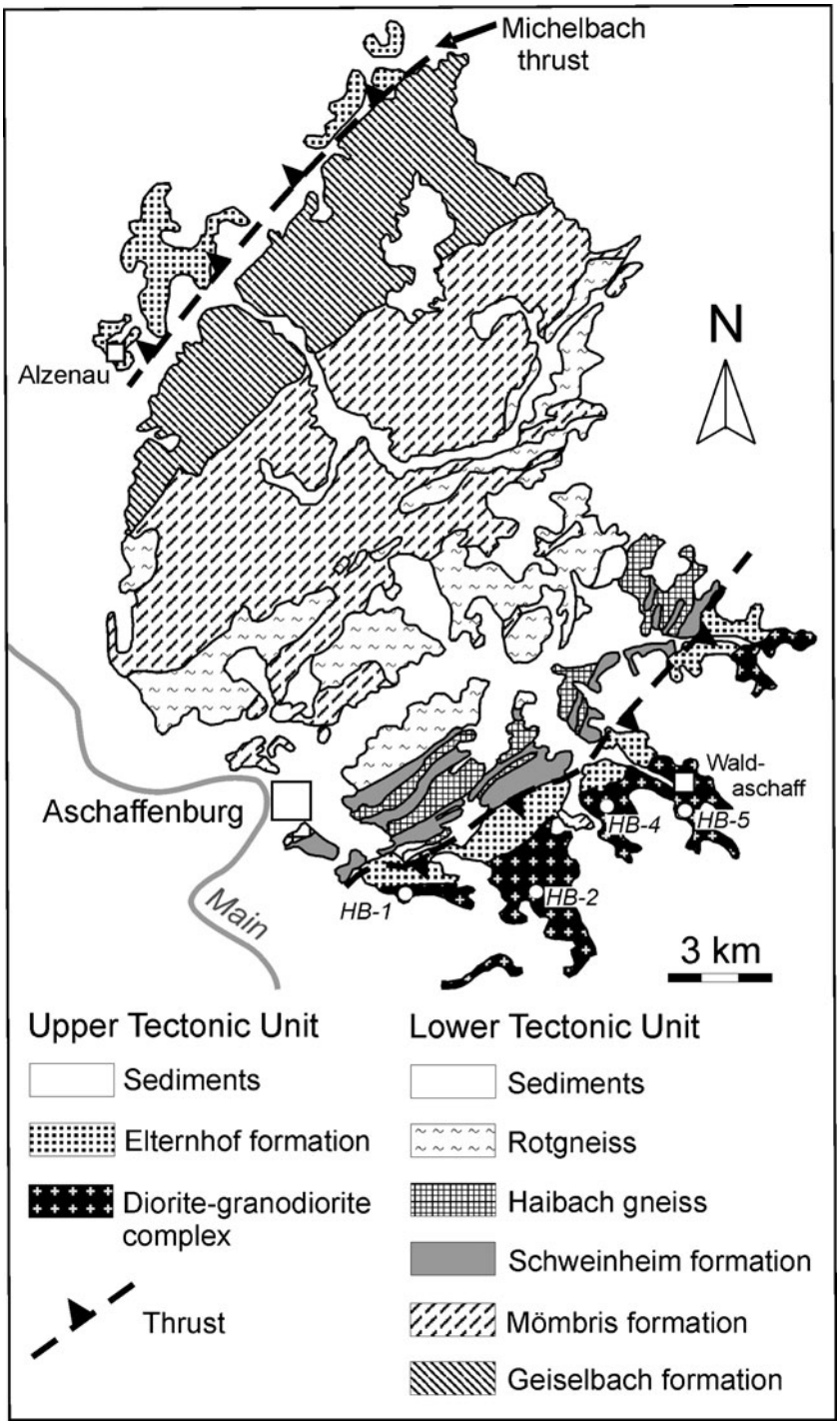

Fig. 3 Spessart crystalline complex (modified after Weber 1995 and Hirschmann and Okrusch 2001) with upper and lower tectonic units and locations of samples from the diorite-granodiorite complex analysed in this study

The Odenwald sample *SEE* comes from a flasergranitoid of unit II, exposed in the Seemann quarry near Hochstädten. Rocks from this quarry show a pronounced planar fabric, which is mainly due to the alignment of mafic minerals (biotite) and feldspar phenocrysts. The NE-SW foliation is steeply inclined and runs parallel to the marginal shear zones and to the main strike direction of unit II that, on a regional scale, is defined by planar mineral fabric and narrow zones of magmatic and metamorphic rocks (Fig. 2). Although the flasergranitoids were interpreted as products of sequential diapirism (Stein 2000, 2001a) it has to be noted that their structures show some deviations from the structures typical for nested diapirs described by Paterson and Vernon (1995). Whereas nested diapirs are normally characterized by concentric foliations and radial orientations of the lineations, unit II granitoids are elongated bodies extending parallel to the orientation of a strike slip zone, which they intrude (Krohe 1991). Foliations in unit II are

Table 1 Sample locations

Spessart diorite-granodiorite complex	
HB-1:	abundant quarry am Stengerts (firing range)
	49° 56′ 50″ N; 9°11′ 23″ E
HB-2:	quarry Stahl, Dörrmorsbach (in use)
	49° 57′ 32″ N; 9°15′ 21″ E
HB-4:	Keilberg
	49° 56′ 46.83″ N, 9°14′13″ E
HB-5:	Waldaschaff
	49° 58′ 05″ N; 9°18′05″ E
Odenwald flasergranitoid	
SEE:	abundant quarry Seemann (renaturated)
	49° 42′ 59″ N; 8° 39′ 41″ E

consistently steep and trend parallel to the extension of the granitoids, and the lineations are horizontal or flatly dipping indicating mainly horizontal mass transfer (Krohe 1992). Therefore it has been argued that the foliation and lineation for the most part reflect the regional strain field associated with strike-slip in addition to deformation induced by the intrusions (for a more comprehensive discussion, see Krohe 1991, 1992, 1994 and Stein 2000, 2001a).

Analytical techniques

For whole-rock geochemistry, samples (2–5 kg each) were crushed in a jaw-crusher and powdered in an agate mill. Major and trace element concentrations were determined by wavelength X-ray fluorescence (XRF) spectrometry on a Bruker AXS S4 pioneer spectrometer. Loss on ignition (LOI) was calculated after heating the sample powder to 1050 °C for 1 h. All elements were measured on fused glass beads made from rock powder (1.50 g) mixed with 7.50 g of Spectromelt fluxing agent and fused at 1150 °C. Certain rare earth elements (i.e., La, Nd, Sm, Eu and Yb), found to be less affected by peak overlap or mass absorption effects, could also be measured on fused glass beads in good accuracy. Rock standards were used to assess the reproducibility and instrument detection limits. Analytical uncertainties range from 1–5 % and 5–10 % for major and trace elements, respectively, depending on the concentration level. For the given rare earth elements detection limits on the order of 5 ppm for La, 0.1 ppm for Eu, 3 ppm for Nd and 0.2 ppm for Yb were achieved. Zircon saturation temperatures were calculated from whole-rock geochemical data by using the experimental model of Watson and Harrison (1983) reviewed in Hanchar and Watson (2003).

For Rb-Sr and Sm-Nd isotope analyses, *c*. 50 mg of whole-rock samples were spiked with ^{87}Rb-^{84}Sr and ^{149}Sm-^{150}Nd mixed tracers, and then dissolved in tightly-capped Teflon PFA vessels with mixtures of HF, HNO_3 and HCl. Strontium and light rare-earth element separation was accomplished on quartz columns by conventional ion exchange chromatography as described previously (Richard et al. 1976). All isotopic measurements were made by Thermal Ionization Mass Spectrometry (TIMS), on a Finnigan MAT 262 mass spectrometer. Strontium was loaded with a tantalum activator (Birck 1986) on pre-conditioned tungsten filaments and measured in single-filament mode. Neodymium was loaded as phosphate on pre-conditioned Rhenium filaments and measurements were performed in a Rhenium double filament assembly. The ^{87}Sr/^{86}Sr isotope ratios were normalised to ^{86}Sr/^{88}Sr=0.1194 and the ^{143}Nd/^{144}Nd isotope ratios to ^{146}Nd/^{144}Nd=0.7219. Analyses of La Jolla Nd-standard gave a ^{143}Nd/^{144}Nd-ratio of 0.511833±0.000009 (n=3) analyses of the NBS 987 Sr-standard yielded a ^{87}Sr/^{86}Sr-ratio of 0.710248±0.000011 (n=3). Total procedural blanks (chemistry and loading) were <250 pg for strontium and <80 pg for neodymium.

Zircons were separated from 125 to 200 μm size fractions by standard mineral separation techniques and were finally hand-picked under a binocular microscope. On the basis of optical microscopy the best quality zircons (free of visible cracks, overgrowths or inclusions) were selected for single-grain U-Pb and Pb-Pb zircon dating.

For isotope dilution TIMS U-Pb analyses, zircons were cleaned with 6N HCl and ultra-pure H_2O and a mixed ^{205}Pb-^{235}U tracer solution was added to the grains prior to dissolution in 22N HF. Separation and purification of uranium and lead were performed in small Teflon columns, filled with 40 μl of Bio-Rad AG1-X8 resin, using standard ion-exchange separation techniques. Uranium and lead isotopic composition was measured on a Finnigan MAT 262 multicollector mass spectrometer on single rhenium filaments using a silica-gel activator. Total procedure blanks were <10 pg for lead and uranium. U-Pb age parameters were calculated using PbDAT and ISOPLOT programs (Ludwig 2003).

Single-zircon Pb-evaporation (Kober 1986, 1987) was performed on a Finnigan MAT 262 mass spectrometer equipped with a MassCom ion counter. From each zircon grain three different temperature steps were measured and the mean of the ^{204}Pb corrected radiogenic ^{207}Pb/^{206}Pb ratios from all steps was calculated following the procedures described in Siebel et al. (2003). The accuracy of the measurements was monitored by repeated measurement of the Plešovice zircon standard which yielded an ^{207}Pb/^{206}Pb evaporation age of 335.3±3.2 Ma (n=5) and an upper intercept U-Pb zircon age of 337.3±2.7 Ma similar to the weighted mean ^{238}U/^{206}Pb age of 337.1±0.4 Ma reported by Sláma et al. (2008).

Results

Petrography and textural characteristics

Sample *SEE* is medium- to coarse-grained with more abundant felsic than mafic components. Thin section microscopy reveals poikilitic plagioclase and microcline phenocrysts enclosing minor opaque oxides, quartz and biotite. Zoned and anti-perthitic plagioclase portrays both Carlsbad and albite twining while microcline is marked by pericline twinning. In places plagioclase and K-feldspar are transformed into epidote. Myrmekitic intergrowths occur between quartz and K-feldspar. Quartz occurs as large and small crystals both marked by undulatory extinction. Nested quartz is characterized by small quartz crystals mantling larger grains. Biotite is the main mafic mineral in sample *SEE*. Greenish biotite microflakes are characteristically interstitial and most are chloritized and occur in association with opaque oxides that are also secondary in nature. Accessories include zircon with marked radiation halos in biotite and apatite. The flasergranitoid sample shows a prominent foliation which is mainly defined by the alignment of biotite. Such fabric, which is common throughout the flasergranitoid zone, indicates solid state deformation in addition to magmatic flow and this deformation locally shows a component of non-coaxial shear consistent with strike slip observed in the wall rocks (Krohe 1991).

The Spessart samples have basically identical mineralogical composition comprising plagioclase, biotite, amphibole and quartz as major phases and titanite, apatite, zircon and opaque oxide accessories. K-feldspar crystals (microcline) may occur in schlieren or in more felsic varieties. Epidote, sericite, chlorite, calcite and hematite/goethite were identified as secondary phases. In detail, the rocks differ by variations in grain size modal proportions of primary minerals and degree of deformation and/or alteration. Sample *HB-1* is medium to coarse grained with an oriented crystalloblastic fabric. Plagioclase is essentially phenocrystic, antiperthitic and poikilitic with biotite, quartz and apatite inclusions. Quartz shows concentric fabric with phenocrystic core and fine mantling grains that formed during dynamic recrystallization. The phenocrysts display undulatory extinction. Hornblende occurs as greenish variety with characteristic basal cleavage and is often in association with yellowish-brown biotite. Zircon is common as inclusions in biotite. Titanite is distinctively idiomorphic. Samples *HB-2* and *HB-4* are medium grained and strongly oriented with mafic minerals defining the fabric and contain abundant plagioclase phenocrysts, large microcline crystals and some quartz. In the altered sample *HB-4* plagioclase is more strongly affected by alteration than microcline. Quartz occurs in nested form with undulatory extinction. Oriented green amphibole and biotite define the foliation of the rocks. Accessory minerals include large idiomorphic titanite, opaque oxides and relatively large zircon grains. Sample *HB-5* shows only slight orientation fabric but is more leucocratic than the other samples due to more abundant felsic minerals. Plagioclase and microcline are characteristically phenocrystic with myrmekitic intergrowths at their contact zones. Large quartz grains display undulatory extinction. Biotite and hornblende constitute the mafic minerals. Some titanite occurrence in association with opaque oxides (magnetite and/or ilmenite) suggests a secondary or late-stage origin.

Geochemistry

Of the investigated samples, four from Spessart are quartz monzodiorite and granodiorite (SiO_2 around 57 wt.%, one sample at 64 wt.%) whereas the Odenwald sample is a more evolved granodiorite with higher silica content (SiO_2=72 wt.%) (Table 2). The Spessart rocks are metaluminous with ASI [= molar $Al_2O_3/(CaO+K_2O+Na_2O)$] ranging from 0.90 to 0.97 whereas the Odenwald sample is marginally peraluminous (ASI=1.02). The rocks belong to the normal- and high-K calc-alkaline series as defined by Peccerillo and Taylor (1976) but also have high sodium resulting in K_2O/Na_2O ratios<1, thus displaying features typical of I-type granites (Chappell and White 2001). TiO_2 (1.1 to 0.7 wt.%), Fe_2O_3 (6.7 to 4.2 wt.%), MgO (3.8 to 2.3 wt.%) and CaO (6.4 to 3.6 wt.%) show considerable variation in the Spessart rocks whereas the Odenwald sample is more depleted in these elements (Table 2). Amongst the trace elements, Sr abundances are as great as 1200 to 1300 ppm, Ba reaches values of 2600 ppm and Zr 250 ppm in some of the Spessart rocks. Again, the Odenwald sample portrays uniformly lower concentrations of these elements. Furthermore, the sample from the Odenwald has lower Rb for the given Sr content than the Spessart samples, a fact that is explained by derivation from largely different (genetically unrelated) parent magmas. Most Spessart samples are characterized by more enhanced LREE/HREE ratios (light rare earth elements/heavy rare earth elements) compared to the Odenwald sample as evidenced by higher La and lower Yb contents (Table 2). The temperature at which zircon starts to crystallize depends on the amount of zirconium present in the melt and this relation can be used as geothermometer (Watson and Harrison 1983). Due to the fact that xenocrystic zircons were not encountered in the investigated intrusions (see next paragraph), the whole-rock data are expected to yield a good approximation for magmatic Zr concentration. Zircon saturation temperatures calculated from bulk rock compositions are between 758 and 786 °C (Table 2).

Table 2 Geochemical composition of granitoids from the Spessart (HB samples) and Odenwald (sample SEE) crystalline complex. Major elements in wt.%, trace elements in ppm. Element concentrations are those measured by X-ray fluorescence, except for Rb, Sr, Sm and Nd which were determined by isotope dilution analyses

	HB1	HB2	HB4	HB5	SEE
SiO_2	56.93	57.02	57.15	63.59	71.89
TiO_2	1.02	1.07	0.95	0.70	0.24
Al_2O_3	18.46	18.22	18.90	16.43	13.75
Fe_2O_3	6.68	5.57	5.41	4.20	2.04
MnO	0.12	0.10	0.10	0.08	0.04
MgO	3.83	3.64	3.34	2.35	0.52
CaO	6.40	5.08	4.63	3.64	2.30
Na_2O	3.88	4.12	4.54	3.84	4.16
K_2O	2.19	3.98	3.60	3.76	2.30
P_2O_5	0.27	0.46	0.40	0.19	0.05
LOI[a]	0.79	1.24	1.10	1.13	0.45
Sum	100.83	100.98	100.58	100.25	97.93
A/CNK	0.97	0.96	0.90	0.91	1.02
K_2O/Na_2O	0.98	0.79	0.97	0.56	0.55
T_{Zr}[b]	758	777	786	766	763
Ba	948	2599	2171	1364	1168
Rb	79	113	106	143	63
Sr	689	1236	1268	811	207
V	147	128	116	81	19
Y	18	8	11	5	6
Zr	194	249	245	159	119
Zn	81	62	67	45	13
Cr	58	56	40	330	0
Ni	88	90	79	202	0
Ce	295	302	314	246	44
La	42	49	67	24	23
Nd	30.6	51.4	59.9	25.0	11.9
Sm	5.7	8.5	9.6	4.1	1.8
Eu	2.4	3.2	3.6	1.9	0.5
Yb	1.7	0.4	0.6	0.4	0.8
La/Yb	25	122	112	60	29
Sr/Y	38	155	115	162	35
Zr/Y	11	32	22	32	20

[a] Loss of ignition

[b] Zircon saturation temperature (°C)

Geochronology

Fifteen zircon grains from four samples of the diorite-granodiorite complex were analysed for their U-Pb isotopic compositions (Table 3). Most grains are prismatic with aspect ratios of 2 to 3. They have moderate to high uranium contents (286–1045 ppm) and relatively high Th/U ratios between 0.38 and 1.43 (Table 3). The data points show a linear decrease from the concordia curve toward the origin as expected for recent lead loss (Fig. 4). There is no evidence for isotopic inheritance in the studied zircon crystals as would be expected for grains containing older resorbed cores. Based on the high U-Pb isotopic closure temperature of zircon (Cherniak and Watson 2001) and lack of pre-magmatic or inherited grains, the upper discordia intercept age of 330.4±2.0 Ma (Fig. 4), which is obtained if the discordia is forced through zero Ma, is regarded as the age of zircon crystallization in the diorite-granodiorite intrusion.

The Pb evaporation technique has been applied to four zircons from the Odenwald flasergranitoid and the $^{207}Pb/^{206}Pb$ ages vary in a narrow range from 330±3.5 to 335±5.6 Ma with a weighted mean age of 332.4±1.6 Ma (Fig. 5, Table 4). Similar $^{207}Pb/^{206}Pb$ ages for different temperature steps as well as similar ages for different grains indicate the absence of a mixed age population or older cores. Th/U values range between 0.16 and 0.36 and are lower than in zircons from the Spessart pluton. The very low $^{204}Pb/^{206}Pb$ ratios (≤0.000061) of all evaporated zircon crystals support the assumption that they were composed of a single concordant homogeneous inclusion-free phase, without significant metamict components. The weighted mean $^{207}Pb/^{206}Pb$ age of 332.4±1.6 Ma is therefore interpreted as crystallization age of the flasergranitoid.

Sr-Nd isotopes

Measured and calculated initial (330 Ma) Rb-Sr and Sm-Nd isotopic compositions are listed in Table 5. Within the Spessart samples, initial $^{87}Sr/^{86}Sr$ values $(^{87}Sr/^{86}Sr)_i$ range from 0.7060 to 0.7066 and $\varepsilon Nd_{(i)}$ values range from −3.0 to −2.3. The Odenwald sample is characterized by a lower $(^{87}Sr/^{86}Sr)_i$ ratio of 0.7049 and a higher $\varepsilon Nd_{(i)}$ value of −0.8. Neodymium model ages (T_{DM}) are 1.32–1.26 Ga for the Spessart diorite-granodiorite complex and 1.14 Ga for the Odenwald flasergranitoid.

Discussion

U-Pb and Pb-Pb analyses of zircons from the southern Spessart diorite-granodiorite complex and a flasergranitoid of the Bergsträsser Odenwald unit II gave virtually identical crystallization ages of 330.4±2.0 and 332.4±1.6 Ma, resp. As far as we are aware there are no published age data on igneous zircons from Odenwald units II and III available for comparison. The new ages fall in the range of previously published K-Ar dating results from these two units (Kreuzer and Harre 1975; Schubert et al. 2001) and also agree with the $^{207}Pb/^{206}Pb$ and K-Ar ages obtained from the Spessart pluton (Nasir et al. 1991; Anthes and Reischmann 2001). The ages apparently postdate the time of the final metamorphism in units II and III of *c*. 336–337 Ma (Todt et al. 1995).

Table 3 U-Pb analytical data from zircons of the Spessart diorite-granodiorite complex

Sample/ Fraction	Weight[a] (mg)	$^{206}Pb/^{204}Pb$	U (ppm)	Pb (ppm)	$^{208}Pb/^{206}Pb$	Th/U[c]	Atomic ratios[d]			Apparent ages (Ma)		
							$^{206}Pb/^{238}U$	$^{207}Pb/^{235}U$	$^{207}Pb/^{206}Pb$	$^{206}Pb/^{238}U$	$^{207}Pb/^{235}U$	$^{207}Pb/^{206}Pb$
HB1-1	0.041	2338	748	38	0.12	0.38	0.04925±26	0.3608±20	0.053139±92	310	313	335
HB1-2	0.037	1467	693	35	0.13	0.41	0.04850±25	0.3555±20	0.053163±111	305	309	336
HB1-3	0.050	2203	549	27	0.12	0.38	0.04849±26	0.3563±21	0.053300±111	305	309	342
HB1-4	0.034	1428	308	16	0.13	0.41	0.04964±25	0.3619±19	0.052879±70	312	314	324
HB2-1	0.033	3496	286	15	0.16	0.51	0.04948±26	0.3617±20	0.053025±68	311	314	330
HB2-2	0.020	3133	379	20	0.15	0.48	0.05026±26	0.3671±19	0.052977±49	316	317	328
HB2-3	0.018	5690	600	31	0.16	0.51	0.04936±27	0.3610±22	0.053048±137	311	313	331
HB2-4	0.026	4154	467	25	0.16	0.51	0.05044±27	0.3689±22	0.053042±124	317	319	331
HB4-1	0.026	3546	453	26	0.17	0.54	0.05321±28	0.3891±21	0.053038±43	334	334	330
HB4-2	0.035	4583	492	27	0.16	0.51	0.05196±29	0.3802±24	0.053070±153	327	327	332
HB4-3	0.037	1963	431	25	0.20	0.63	0.05268±27	0.3852±20	0.053032±47	331	331	330
HB4-4	0.011	6477	612	35	0.17	0.54	0.05335±34	0.3910±34	0.053157±280	335	335	336
HB5-1	0.019	105	1291	96	0.45	1.43	0.04302±23	0.3148±22	0.053062±219	272	278	331
HB5-2	0.035	293	942	58	0.22	0.70	0.05026±27	0.3680±22	0.053106±109	316	318	333
HB5-3	0.023	154	1045	69	0.34	1.08	0.04547±28	0.3331±31	0.053135±328	287	292	335

[a] Error for weight and concentration <20 %

[b] Measured ratios corrected for mass fractionation and tracer contribution

[c] Calculated from time-integrated $^{232}Th/^{238}U$ values, present-day $^{208}Pb/^{206}Pb$ ratios and the respective $^{207}Pb/^{206}Pb$ age

[d] Corrected for blank contribution lead, uranium, and initial lead composition with $^{206}Pb/^{204}Pb=18.20$, $^{207}Pb/^{204}Pb=15.60$; errors are $2\sigma_m$

However, there is evidence that zircon crystallization occurred late during magma evolution (see next paragraph). Overall, the zircon ages are coherent with the model of melt intrusion during final metamorphic stages related to Variscan collisional tectonics between Avalonia and Armorica.

Isotopic characteristics and distribution of uranium and thorium can be used to determine the crystallization conditions

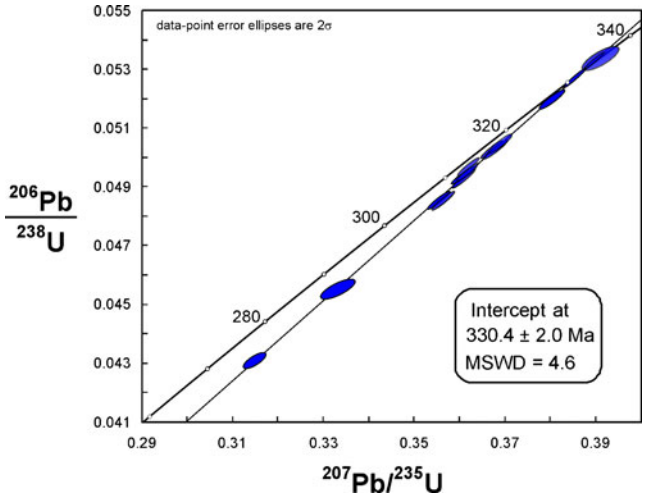

Fig. 4 U-Pb concordia diagram showing the results of isotope dilution TIMS dating of fifteen zircon fractions from four samples of the Spessart diorite-granodiorite complex. A 330.4±2 Ma upper intercept age is obtained if the results are forced by a discordia through zero (representing recent lead loss)

of zircon. It is known from empirical observation that magmatic zircons generally have higher Th/U ratios (>0.1) compared to metamorphic grains (e.g., Hoskin and Ireland 2000). Although a high Th/U alone is no clear proof for igneous zircon growth (e.g., Möller et al. 2002, 2003; Harley et al. 2007), a clean metamorphic signature (i.e. extremely low Th/U ratios) is not found in any of our investigated zircon grains (Tables 3 and 4). Zircons from both investigated rock units are characterized by high Th/U ratios (Spessart: $Th/U_{Zircon}=0.38$–1.43, Odenwald: $Th/U_{zircon}=0.16$–0.36) in accordance with crystallization from a melt (Hoskin and Ireland 2000). Moreover, the higher Th/U ratios of the Spessart zircons are in agreement with their precipitation from a more mafic magma composition (Xiang et al. 2011) and this interpretation is supported by bulk-rock geochemical data (Table 2). Lack of perceptible zircon cores (no pre-magmatic ages as evidenced from U-Pb and $^{207}Pb/^{206}Pb$ evaporation ages) is consistent with magma generation above the zircon saturation temperature. Taking into account the deep emplacement level that has been inferred for the granitoids from barometric investigations (Willner et al. 1991; Altherr et al. 1999), the low zircon saturation temperatures (Table 2) argue against zircon crystallization at magmatic liquidus temperatures. Results from other studies present evidence that the temperatures obtained by the Ti-in-zircon thermometer can significantly (about 50–100 °C) underestimate the onset temperature of zircon crystallization in an initially zircon-undersaturated magma (Miller et al. 2003;

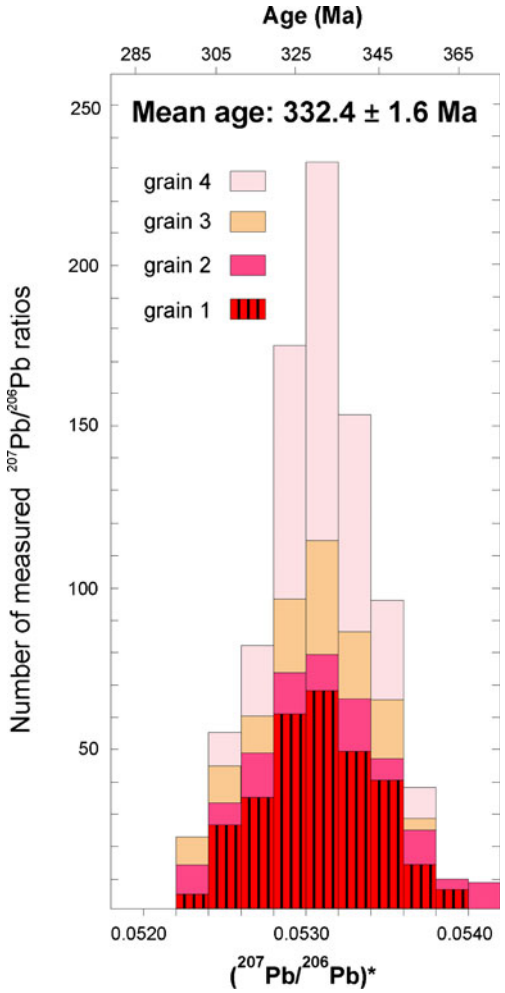

Fig. 5 Histogram showing the distribution of radiogenic $^{207}Pb/^{206}Pb$ ratios obtained from stepwise evaporation of four zircon grains from sample *SEE* (Bergsträsser Odenwald, unit II). The $^{207}Pb/^{206}Pb$ age for all zircons is given as weighted average and the error refers to the 95 % confidence level

Kemp et al. 2005; Harrison et al. 2007). Thus, we think that the calculated temperatures for the Spessart and Odenwald magmas do not reflect the initial melt temperatures. Given the above arguments it seems likely that the magmas were undersaturated and that zircon crystallization occurred after a notable temperature drop. It is also likely that a combination of local constraints like tectonic environment (syn-collisional tectonic setting, metamorphic hydration reactions), emplacement in a hot crustal zone and/or mafic composition of the parental melt affected crystallization behaviour of zircon. In such a scenario a replacement of early crystallized zircon by a coupled dissolution-reprecipitation process (Putnis 2002) could have been occurred. In such a case dissolution of feldspar could have changed the chemical composition and alkalinity of fluids affecting the solubility of zircon during synkinematic pluton deformation (e.g., Geisler et al. 2007). In summary, the zircon ages may either reflect late magmatic growth, or reaction processes during the presence of a late-magmatic or metamorphic fluid.

In the following the relationship between Spessart diorite-granodiorite complex and granitoids from the Odenwald will be explored. Odenwald unit II shows a correlated distribution from more basic to intermediate diorites in the south to more acidic granodiorites and granites in the north, opposite to the general zonation of the Bergsträsser Odenwald (Stein 2001b). The analysed flasergranitoid sample *SEE* represents a felsic granite variety of unit II. This sample corresponds to the felsic NMS (Neunkirchen magmatic suite) described in Altherr et al. (1999). Compared to the Spessart diorite-granodiorite complex, the Odenwald flasergranitoid shows a much higher degree of chemical evolution (Table 2). Yet, it has to be explored if the Spessart complex is genetically related to the more mafic magmatic suite of Odenwald unit II, or approximates a potential mafic parent magma composition for the investigated flasergranitoid. Samples from the Spessart complex have a relative evolved isotope composition and this makes any genetic relationship to the flasergranitoid of unit II unlikely. To address this question in more detail we have included literature data from granitoids of unit II and III

Table 4 $^{207}Pb/^{206}Pb$ evaporation data for single zircons from the Odenwald flasergranitoid

Sample/Grain no.	No[a]	$^{204}Pb/^{206}Pb$	$^{208}Pb/^{206}Pb$	Th/U[b]	$^{207}Pb/^{206}Pb$[c]	$^{207}Pb/^{206}Pb$ age (Ma)	Error (Ma)[d]
SEE							
1	306	0.000040	0.109	0.34	0.053077±40	332.1	2.9
2	119	0.000010	0.110	0.35	0.053146±118	335.1	5.6
3	137	0.000061	0.053	0.17	0.053027±61	330.0	3.5
4	336	0.000021	0.049	0.16	0.053107±27	333.4	2.6
Weighted average						332.4	1.6

[a] Number of measured $^{207}Pb/^{206}Pb$ isotope ratios per grain

[b] Calculated from time-integrated $^{232}Th/^{238}U$ values, present-day $^{208}Pb/^{206}Pb$ ratios and the respective $^{207}Pb/^{206}Pb$ age

[c] ±2σ standard deviation

[d] Error calculated using following formulae: $\sqrt{(2\sigma/\sqrt{n})^2 + \Delta f^2}$, where n is the number of measured $^{207}Pb/^{206}Pb$ isotope ratios, 2σ is the 2-sigma standard error of the Gaussian frequency distribution function and ΔF is an assumed uncertainty of the measured $^{207}Pb/^{206}Pb$ ratio of 0.1 %

Table 5 Rb-Sr and Sm-Nd analytical data together with εNd values and T_{DM} model ages for granitoids from the Spessart and Odenwald crystalline complex

Sample	$^{87}Rb/^{86}Sr$	$^{87}Sr/^{86}Sr$[a]	$(^{87}Sr/^{86}Sr)_i$[b]	$^{147}Sm/^{144}Nd$	$^{143}Nd/^{144}Nd$[a]	$(^{143}Nd/^{144}Nd)_i$[b]	$\varepsilon Nd_{(t)}$[c]	T_{DM}(Ga)[d]
Spessart								
HB-1	0.3334	0.707545±10	0.70598	0.1126	0.512304±9	0.512060	−3.0	1.32
HB-2	0.2650	0.707692±9	0.70645	0.1004	0.512313±9	0.512096	−2.3	1.26
HB-4	0.2408	0.707527±10	0.70640	0.0964	0.512279±9	0.512070	−2.8	1.30
HB-5	0.5110	0.709015±10	0.70661	0.0991	0.512304±9	0.512090	−2.4	1.27
Odenwald								
SEE	0.8789	0.708983±8	0.70485	0.0933	0.512375±9	0.512173	−0.8	1.14

[a] Errors are $2\sigma_{measured}$

[b] Initial ratios calculated using the age 330 ma

[c] Typical uncertainty in $\varepsilon Nd_{(t)}$ (t=330 Ma) is ±0.4

[d] Nd depleted mantle model age (two-stage) with parameters given in Liew and Hofmann (1988)

(Altherr et al. 1999). As can be seen from Fig. 6, the flasergranitoid sample *SEE* plots well within the range of other granitoids of unit II. Felsic granitoids of unit II have low values of Sr/Y and Zr/Y (Altherr et al. 1999), which is also a characteristic feature of sample *SEE* (Table 2). On the other hand, there is a large overlap in initial Sr and Nd isotope ratios between the Spessart diorite-granodiorite complex and Odenwald granitoids from unit III (Fig. 6). This finding is sustained by the similarity of other geochemical parameters (Table 2, Fig. 3 in Altherr et al. 1999). For example, Sr/Y and Zr/Y ratios are high in the Spessart complex similar to those in Odenwald unit III granitoids (Weschnitz, Tromm and Heidelberg). As pointed out by Altherr et al. (1999) the isotopic and compositional differences between the Odenwald granitoids of unit I, II and III are related to different source rocks or different depth of melt production. We consider it most likely that the flasergranitoid of unit II

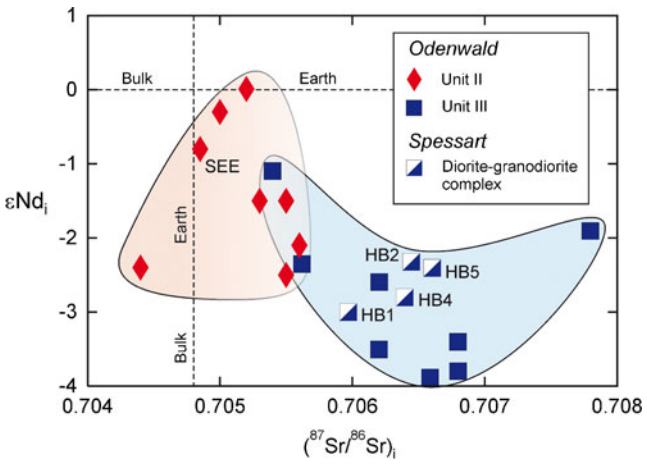

Fig. 6 Sr-Nd isotope correlation diagram for granitoids from the Spessart and Odenwald analysed in this study (i.e., sample *SEE* and samples *HB-1, HB-2, HB-4* and *HB-5*) compared with literature data from the Odenwald units II and III (Altherr et al. 1999)

was derived from young or isotopically primitive (i.e., low Sr and high εNd signatures) hot immature crust, or from a hybrid (mantle + crust) source, followed by extensive subsequent internal fractional crystallization of amphibole, feldspar, Fe-Ti oxides and apatite. In contrast, the higher initial Sr and lower εNd values and the high Sr/Y and Zr/Y ratios for those from Odenwald unit III suggest melt derivation from a garnet-bearing lower crustal source (Altherr et al. 1999). The similar compositional characteristics between unit III granitoids and the Spessart diorite-granodiorite complex would thus allow essentially identical lower crustal sources.

Conclusions

Geochronological data obtained during this study show that the southern Spessart and Bergsträsser Odenwald unit II, as parts of the Armorican-type MGCR, host granitoids with virtually identical average zircon ages (330–332 Ma). Parental magmas solidified deep within the crust during syn-collisional process and were undersaturated in Zr preventing early zircon precipitation or zircon crystallization was controlled by dissolution-reprecipitation processes. The felsic (SiO_2-rich) Odenwald granitoid is isotopically more primitive than the mafic-intermediate Spessart complex. In conjunction with geochemical data (Rb/Sr, Sr/Y, Zr/Y ratios), this suggests fundamentally differences in magma generation processes and/or parent magma composition in the southern Spessart and Odenwald unit II. On the other hand, the chemical and isotope signatures of unit III plutons are more akin to the Spessart granitoid complex than to any other unit from the Odenwald. Hence, it is concluded that the diorite-granodiorite complex of the southern Spessart constitutes the north-eastern extension of Bergsträsser Odenwald unit III.

Acknowledgements This work was supported by a grant from the Landesamt für Umwelt, Augsburg. We thank Elmar Reitter and Heiner Taubald for support during XRF, Rb-Sr and Sm-Nd isotope analyses. Alexander Krohe, Andreas Möller and an anonymous referee provided constructive comments and suggestions that helped to improve the manuscript.

References

Allen CM (1993) A nested diapir model for the reversely zone Turtle pluton, southeastern California. Trans R Soc Edinb Earth Sci 83:179–190

Altherr R, Henes-Klaiber U, Hegner E, Satir M, Langer C (1999) Plutonism in the Variscan Odenwald (Germany): from subduction to collision. Int J Earth Sci 88:422–443

Anthes G, Reischmann T (2001) Timing of granitoid magmatism in the eastern mid-German crystalline rise. J Geodynamics 31:119–143

Bederke E (1957) Alter und Metamorphose des kristallinen Grundgebirges im Spessart. Abh Hess L-Amt Bodenforsch 18:7–19

Behr HJ, Heinrichs T (1987) Geological interpretation of DEKORP 2-S: a deep seismic reflection profile across the Saxothuringian and possible implications for the late Variscan structural evolution of central Europe. Tectonophysics 142:173–202

Birck JL (1986) Precision K–Rb–Sr isotopic analysis: application to Rb–Sr chronology. Chem Geol 56:73–83

Braitsch O (1957a) Beitrag zur Kenntnis der kristallinen Gesteine des südlichen Spessarts und ihrer geologisch-tektonischen Geschichte. Abh Hess L-Amt Bodenforsch 18:21–72

Braitsch O (1957b) Zur Petrographie und Tektonik des Biotitgneises im südlichen Vorspessart. Abh Hess L-Amt Bodenforsch 18:73–99

Chappell BW, White AJR (2001) Two contrasting granite types: 25 years later. Austr J Earth Sci 48:489–499

Cherniak DJ, Watson EB (2001) Pb diffusion in zircon. Chem Geol 172:5–24

Dombrowski A, Okrusch M, Henjes-Kunst F (1994) Geothermobarometry and geochronology on mineral assemblages of orthogneisses and related metapelites of the Spessart crystalline complex, NW Bavaria, Germany. Chem Erde 54:85–101

Dombrowski A, Henjes-Kunst F, Höhndorf A, Kröner A, Okrusch M, Richter P (1995) Orthogneisses in the Spessart crystalline complex, North-West Bavaria—Silurian granitoid magmatism at an active continental-margin. Geol Rdsch 84:399–411

Faure M, Sommers C, Melleton J, Cocherie A, Lautout O (2010) The Léon domain (French massif Armoricain): a westward extension of the mid-German crystalline rise? Structural and geochronological insights. Int J Earth Sci 99:65–81

Finger F, Roberts MP, Haunschmid B, Schermaier A, Steyrer HP (1997) Variscan granitoids of central Europe: their typology, potential sources and tectonothermal relations. Mineral Petrol 61:67–96

Franke W (2000) The mid European segment of the Variscides: tectono-stratigraphic units, terrane boundaries and plate tectonic evolution. In: Franke W, Haak V, Oncken O, Tanner D (eds) Orogenic processes: quantification and modelling in the Variscan belt: Geol Soc London Spec Publ 179:35–62

Geisler T, Schaltegger U, Tomaschek F (2007) Re-equilibration of zircon in aqueous fluids and melts. Elements 3:43–50

Hanchar JM, Watson EB (2003) Temperature saturation temperature. In: Hanchar JM, Hoskin PWO (eds) Zircon: Rev Mineral Geochem 53:89–112

Hann HP, Chen F, Zedler H, Frisch W, Löschke J (2003) The Rand granite in the southern Schwarzwald and its geodynamic significance in the Variscan belt of SW Germany. Int J Earth Sci 92:821–842

Harley SL, Kelly M, Möller A (2007) Zircon behaviour and the thermal histories of mountain chains. Elements 3:25–30

Harrison TM, Watson EB, Aikman AB (2007) Temperature spectra of zircon crystallization in plutonic rocks. Geology 35:635–638

Henes-Klaiber U (1992) Zur Geochemie der Variscischen Granitoide des Bergsträsser Odenwaldes. PhD Thesis Univ Karlsruhe 264 pp

Hirschmann G, Okrusch M (2001) Spessart unf Rhön (18)—Teil der MKZ. In: Stratigraphie von Deutschland II. Ordovizium, Kambrium, Vendium, Riphäikum. Teil II: Baden-Württemberg, Bayern, Hessen, Rheinland-Pfalz, Nordthüringen, Sachsen-Anhalt, Brandenburg. Courier Forschungsinstitut Senckenberg (CFS) 234:93–108

Hoskin PWO, Ireland TR (2000) Rare earth element chemistry of zircon and its use as a provenance indicator. Geology 28:627–630

Kemp A, Whitehouse M, Hawkesworth C, Alarcon M (2005) A zircon U-Pb study of metaluminous (I-type) granites of the Lachlan fold belt, southeastern Australia: implications for the high/low temperature classification and magma differentiation processes. Contrib Mineral Petrol 150:230–249

Kirsch H, Kober B, Lippolt HJ (1988) Age of intrusion and rapid cooling of the Frankenstein gabbro (Odenwald, SW-Germany) evidenced by $^{40}Ar/^{39}Ar$ and single-zircon $^{207}Pb/^{206}Pb$ measurements. Geol Rdsch 77:693–711

Kober B (1986) Whole-grain evaporation for $^{207}Pb/^{206}Pb$-age-investigations on single zircons using a double-filament thermal ion-source. Contrib Mineral Petrol 93:482–490

Kober B (1987) Single-zircon evaporation combined with Pb^{+} emitter bedding for $^{207}Pb/^{206}Pb$-age investigations using thermal ion mass-spectrometry, and implications to zirconology. Contrib Mineral Petrol 96:63–71

Kreher B (1994) Petrologie und Geochemie der Gabbrointrusionen des Frankensteins (Odenwald). Geol Jb Hessen 122:81–122

Kreuzer H, Harre W (1975) K/Ar-Altersbestimmungen an Hornblenden und Biotiten des kristallinen Odenwaldes. Aufschluss 27:71–78

Krohe A (1991) Emplacement of synkinematic plutons in the Variscan Odenwald (Germany) controlled by transtensional tectonics. Geol Rdsch 80:391–409

Krohe A (1992) Structural evolution of intermediate-crustal rocks in a strike-slip and extensional setting (Variscan Odenwald, SW Germany)—differential upward transport of metamorphic complexes and changing deformation mechanisms. Tectonophysics 205:357–386

Krohe A (1994) Verformungsgeschichte in der mittleren Kruste eines magmatischen Bogens, - der variszische Odenwald als Modellregion. Geotekt Forsch 80:1–147

Krohe A (1996) Variscan tectonics of central Europe: postaccretionary intraplate deformation of weak continental lithosphere. Tectonics 15:1364–1388

Kroner U, Mansy J-L, Mazur S, Aleksandrowski P, Hann HP, Huckriede H, Lacquement F, Lamarche J, Ledru P, Pharaoh TC, Zedler H, Zeh A, Zulauf G (2008) Variscan tectonics. In: McCann T (ed) The geology of Central Europe, vol. 1. Geological Society, London, pp 599–664

Liew TC, Hofmann AW (1988) Precambrian crustal components, plutonic associations, plate environment of the Hercynian fold belt of central-Europe—indications from a Nd and Sr isotopic study. Contrib Mineral Petrol 98:129–138

Linnemann U, McNaughton N, Romer R, Gehmlich M, Drost K, Tonk C (2004) West African provenance for Saxo-Thuringia (Bohemian Massif): did Armorica ever leave pre-Pangean Gondwana?—U/Pb-SHRIMP zircon evidence and the Nd-isotopic record. Int J Earth Sci 93:683–705

Lippolt HJ (1986) Nachweis altpaläozoischer Primäralter (Rb-Sr) und karbonischer Abkühlalter (K-Ar) der Muskovit-Biotit-Gneise des Spessarts und der Biotit-Gneise des Böllsteiner Odenwaldes. Geol Rdsch 75:569–583

Ludwig KR (2003) User's manual for Isoplot 3.00 a geochronological toolkit for Microsoft Excel

McKerrow WS, Ziegler AM (1972) Palaeozoic oceans. Nature Phys Sci 240:92–94

Miller CF, McDowell SM, Mapes RW (2003) Hot and cold granites? Implications of zircon saturation temperatures and preservation of inheritance. Geology 31:529–532

Möller A, O'Brien PJ, Kennedy A, Kröner A (2002) Polyphase zircon in ultrahigh-temperature granulites (Rogaland, SW Norway): constraints for Pb diffusion in zircon. J Metamorph Geol 20:727–740

Möller A, O'Brien PJ, Kennedy A, Kröner A (2003) Linking growth episodes of zircon and metamorphic textures to zircon chemistry: an example from the ultrahigh temperature granulites of Rogaland (SW Norway). In: Vance D, Müller W, Villa IM (eds) Geochronology: Linking the isotopic record with petrology and textures: Geol Soc London Spec Publ 220:65–81

Nance RD, Gutiérrez-Alonso G, Keppie JD, Linnemann U, Murphy JB, Quesada C, Strachan RA, Woodcock NH (2010) Evolution of the Rheic ocean. Gondw Res 17:194–222

Nasir S, Okrusch M, Kreuzer H, Lenz H, Höhndorf A (1991) Geochronology of the Spessart crystalline complex, mid-German crystalline rise. Mineral Petrol 44:39–55

Nickel E, Maggetti M (1974) Magmengenese und Dioritbildung im synorogen konsolidierten Grundgebirge des Bergsträßer Odenwaldes. Geol Rdsch 63:618–654

Okay AI, Satir M, Siebel W (2006) Pre-Alpine and Mesozoic orogenic events in the eastern Mediterranean region. In: Gee DG, Stephenson RA (eds) European lithosphere dynamics. Geol Soc London, Mem 32:389–405

Okay N, Zack T, Okay AI, Barth M (2011) Sinistral transport along the Trans-European suture zone: detrital zircon-rutile geochronology and sandstone petrography from the Carboniferous flysch of the Pontides. Geol Mag 148:380–403

Okrusch M (1963) Bestandsaufnahme und Deutung dioritartiger Gesteine im südlichen Vorspessart. Ein Beitrag zum Dioritproblem. Geol Bavarica 51:4–107

Okrusch M, Richter P (1986) Orthogneisses of the Spessart crystalline complex, northwest Bavaria—indicators of the geotectonic environment. Geol Rdsch 75:555–568

Okrusch M, Geyer G, Lorenz J (2011) Spessart. Sammlung geol Führer 106:1–368

Oncken O (1997) Transformation of a magmatic arc and an orogenic root during oblique collision and its consequences for the evolution of the European Variscides. Geol Rdsch 86:2–20

Oncken O (1998) Evidence for precollisional subduction erosion in ancient collisional belts: the case of the mid-European Variscides. Geology 26:1075–1078

Paterson SR, Vernon RH (1995) Bursting the bubble of ballooning plutons: a return to nested diapirs emplaced by multiple processes. Geol Soc Am Bull 107:1356–1380

Peccerillo A, Taylor SR (1976) Geochemistry of Eocene calcalkaline volcanic rocks from the Kastamonu area, northern Turkey. Contrib Mineral Petrol 58:63–81

Pin C, Paquette JL (2002) Le magmatisme basique calcoalcalin d'âge dévono–dinantien du nord du Massif Central, témoin d'une marge active hercynienne: arguments géochimiques et isotopiques Sr/Nd. Geodinamica Acta 15:63–77

Poller U, Janak M, Kohut M, Todt W (2000) Early Variscan magmatism in the western Carpathians: U-Pb zircon data from granitoids and orthogneisses of the Tatra mountains (Slovakia). Int J Earth Sci 89:336–349

Putnis A (2002) Mineral replacement reactions: from macroscopic observations to microscopic mechanisms. Mineral Mag 66:689–708

Richard P, Shimizu N, Allègre CJ (1976) $^{143}Nd/^{144}Nd$, a natural tracer: an application to oceanic basalts. Earth Planet Sci Lett 31:269–278

Schälicke W (1975) Die Otzberg-Zone. Aufschluß Sonderbd 27:47–57

Schaltegger U (1997) Magma pulses in the central Variscan belt: episodic melt generation and emplacement during lithospheric thinning. Terra Nova 9:242–245

Scherer EE, Mezger K, Münker C (2002) Lu-Hf ages of high pressure metamorphism in the Variscan fold belt of southern Germany. Geochim Cosmochim Acta 66:A677

Schubert W, Lippolt HJ, Schwarz W (2001) Early to middle Carboniferous hornblende $^{40}Ar/^{39}Ar$ ages of amphibolites and gabbros from the Bergsträsser Odenwald. Mineral Petrol 72:113–132

Shaw A, Downes H, Thirlwall MF (1993) The quartz-diorites of Limousin: elemental and isotopic evidence for Devono-Carboniferous subduction in the Hercynian belt of the French Massif Central. Chem Geol 107:1–18

Siebel W (1998) Variszischer spät-bis postkollisionaler Plutonismus in Deutschland: Regionale Verbreitung, Stoffbestand und Altersstellung. Z Geol Wiss 26:329–358

Siebel W, Chen F, Satir M (2003) Late Variscan magmatism revisited: new implications from Pb-evaporation zircon ages on the emplacement of redwitzites and granites in NE Bavaria. Int J Earth Sci 92:36–53

Sláma J, Košler J, Condon DJ, Crowley JL, Gerdes A, Hanchar JM, Horstwood MSA, Morris GA, Nasdala L, Norberg N, Schaltegger U, Schöne B, Tubrett MN, Whitehouse MJ (2008) Plesovice zircon—a new natural reference material for U-Pb and Hf isotopic microanalysis. Chem Geol 249:1–35

Stampfli GM, von Raumer JF, Borel GD (2002) Paleozoic evolution of pre-Variscan terranes: from Gondwana to the Variscan collision. Geol Soc Am Spec Pap 364:263–280

Stein E (2000) Zur Platznahme von Granitoiden – vergleichende Fallstudien zu Gefügen und Platznahmemechanismen aus den White-Inyo Mountains, California, USA, und dem Bergsträßer Odenwald. Geotektonische Forschungen 93:1–344

Stein E (2001a) Die magmatischen Gesteine des Bergsträßer Odenwaldes und ihre Platznahme-Geschichte. Jber Mitt oberrhein geol Ver NF 83:267–283

Stein E (2001b) The geology of the Odenwald crystalline complex. Mineral Petrol 72:7–28

Timmerman MJ (2008) Palaeozoic magmatism. In: McCann T (ed) The geology of central Europe, vol 1: Precambrian and Palaeozoic. Geol Soc London, 665–748

Todt WA, Altenberger U, von Raumer JF (1995) U-Pb data on zircons for the thermal peak of metamorphism in the Variscan Odenwald, Germany. Geol Rdsch 84:466–472

Watson EB, Harrison TM (1983) Zircon saturation revisited—temperature and composition effects in a variety of crustal magma types. Earth Planet Sci Lett 64:295–304

Weber K (1995) The Spessart crystalline complex. In: Dalmeyer R, Franke W, Weber K (eds) Pre-Permian geology of central and eastern Europe. Springer, Berlin, pp 167–173

Will TM, Schmädicke E (2001) A first find of retrogressed eclogues in the Odenwald crystalline complex, mid-German crystalline rise, Germany: evidence for a so far unrecognised high-pressure metamorphism in the central Variscides. Lithos 59:109–125

Will TM, Schmädicke E (2003) Isobaric cooling and anti-clockwise P-T paths in the Variscan Odenwald crystalline complex, Germany. J Metamorph Geol 21:469–480

Willner AP, Massonne HJ, Krohe A (1991) Tectonothermal evolution of a part of a Variscan magmatic arc—the Odenwald in the mid-German crystalline rise. Geol Rdsch 80:369–389

Xiang W, Griffin WL, Jie C, Pinyun H, Xiang LI (2011) U and Th contents and Th/U ratios of zircon in felsic and mafic magmatic rocks: improved zircon-melt distribution coefficients. Acta Geol Sin 85:164–174

Žák J, Kratinová Z, Trubač J, Janoušek V, Sláma J, Mrlina J (2010) Structure, emplacement, and tectonic setting of late Devonian granitoid plutons in the Teplá–Barrandian unit, Bohemian Massif. Int J Earth Sci. doi:10.1007/s00531-010-0565-7

Zeh A, Will TM (2010) The mid-German crystalline zone. In: Linnemann U, Romer R (eds) Pre-Mesozoic geology of Saxo-Thuringia—from the Cadomian active margin to the Variscan Orogen. Schweitzerbart, Stuttgart, pp 195–220

Zeh A, Gerdes A, Will TM, Millar IL (2005) Provenance and magmatic-metamorphic evolution of a Variscan island-arc complex: constraints from U-Pb dating, petrology, and geospeedometry of the Kyffhäuser crystalline complex, central Germany. J Petrol 46:1393–1420